

Lattice Parameter Variation in ScGaN Alloy Thin Films on MgO(001) Grown by RF Plasma Molecular Beam Epitaxy

Costel Constantin¹, Jeongihm Pak², Kangkang Wang², Abhijit Chinchore², Meng Shi², and Arthur R. Smith²

¹Department of Physics, Seton Hall University, South Orange, NJ 07079

²Nanoscale & Quantum Phenomena Institute, Department of Physics and Astronomy, Ohio University, Athens, OH 45701

ABSTRACT

We present the structural and surface characterization of the alloy formation of scandium gallium nitride $\text{Sc}_x\text{Ga}_{1-x}\text{N}(001)/\text{MgO}(001)$ grown by radio-frequency molecular beam epitaxy over the Sc range of $x = 0-100\%$. In-plane diffraction measurements show a clear face-centered cubic surface structure with single-crystalline epitaxial type of growth mode for all x ; a diffuse/distinct transition in the surface structure occurs at near $x = 0.5$. This is consistent with out-of-plane diffraction measurements which show a linear variation of perpendicular lattice constant a_{\perp} for $x = 0$ to 0.5 , after which a_{\perp} becomes approximately constant. The $x = 0.5$ transition is interpreted as being related to the cross-over from zinc-blende to rock-salt structure.

INTRODUCTION

The technological achievement of light emitting diodes (LEDs) made out of wurtzite GaN (w-GaN) spurred much interest in related III-nitrides such as aluminium nitride (AlN) and indium nitride (InN). Wurtzite GaN has a band gap of 3.4 eV and emits invisible, highly energetic ultraviolet light, but when some of the gallium atoms are substituted by indium atoms, highly efficient violet, or blue LEDs can be obtained. However, alloying w-GaN with AlN or InN has shown a decrease in device efficiency as the emission wavelength is shifted towards the near infrared-end of the visible spectrum. A very good alternate to w-GaN is the cubic GaN (c-GaN) which has several interesting properties such as a direct wide band gap of $E_D^{c\text{-GaN}} = 3.2 \text{ eV}$, a tetrahedral zinc-blende bonding structure with a lattice constant of $a_{c\text{-GaN}} = 0.452 \text{ nm}$ [1, 2]. On the other hand, scandium nitride (ScN) is a semiconductor with a direct band gap of $E_D^{\text{ScN}} = 2.15 \text{ eV}$ and a lower indirect band gap of $E_I^{\text{ScN}} = 0.9 \text{ eV}$ [3-7]. The most stable crystal structure of ScN observed experimentally so far is the rock-salt structure with a relaxed lattice constant $a_{\text{ScN}} = 0.4501 \text{ nm}$ [6]. It can be noticed that there is $\sim 0.2\%$ lattice constant mismatch between c-GaN and ScN, and also the different bandgaps [i.e., c-GaN (3.2 eV), and ScN (2.15 eV)] makes ScGaN alloying and the growth of c-GaN/ScN and ScN/c-GaN extremely appealing. We previously reported the growth of $\text{Sc}_x\text{Ga}_{1-x}\text{N}$ on wurtzite GaN, and we found that for both low x and high x , alloy-type behavior is observed. For $x \geq 0.54$, rock-salt structure is found; for small x up to 0.17, an anisotropic expansion of the ScGaN lattice is observed which is interpreted in terms of local lattice distortions of the wurtzite structure in the vicinity of Sc_{Ga} substitutional sites in which there is a decrease of the N-Sc-N bond angle. This tendency toward flattening of the wurtzite bilayer is consistent with a predicted h -ScN phase [8-10].

So far there are no experimental reports regarding the growth of the ScGaN on substrates with a cubic symmetry [i.e., MgO(001)]. In this article we explore the growth of ScGaN on MgO(001) substrates by radio-frequency plasma-assisted molecular beam epitaxy (rf-MBE). We grew a set of five films of $\text{Sc}_x\text{Ga}_{1-x}\text{N}(001)/\text{MgO}(001)$ with $x = 0-1$ in increments of 0.25. The films are measured *in-situ* with reflection high-energy electron diffraction (RHEED) which has a 20 keV electron beam, and *ex-situ* by x-ray diffraction (XRD) which has Cu $K_{\alpha 1}$ and $K_{\alpha 2}$ x-rays.

EXPERIMENT

The growth experiments are performed in a homemade radio-frequency plasma molecular beam epitaxy (rf-plasma MBE) utilizing gallium and scandium effusion cells. The N_2 gas was delivered through an rf-plasma source; the N_2 flow rate and rf-plasma power were maintained constant throughout the entire growth at 1.1 sccm ($P_{\text{chamber}} = 9 \times 10^{-6}$ Torr) and 500 Watts, respectively. Growth was performed on MgO(001) substrates which were ultrasonically cleaned with acetone and isopropanol, after which they were loaded into the MBE chamber and prepared by heating and nitridation at a temperature of $\sim 900^\circ\text{C}$ for 30 minutes, while keeping the N_2 flow rate to 1.1 sccm and the rf-plasma power at 500 W. The ScGaN films were then grown at a substrate temperature of $\sim 900^\circ\text{C}$ and a flux ratio $r = J_{\text{Sc}} / (J_{\text{Sc}} + J_{\text{Ga}})$ and to a thickness of 80 – 495 nm. The Sc and Ga fluxes were $f_{\text{Sc}} = 0 - 2.2 \times 10^{14} / (\text{cm}^2 \text{ sec})$, and $f_{\text{Ga}} = 0 - 5.8 \times 10^{14} / (\text{cm}^2 \text{ sec})$. The sum of metal fluxes, $f_{\text{Sc}} + f_{\text{Ga}}$, for each film was within the range $2.2 - 7.7 \times 10^{14} / (\text{cm}^2 \text{ sec})$.

RESULTS AND DISCUSSIONS

Figure 1(a) – (j) show RHEED patterns of $\text{Sc}_x\text{Ga}_{1-x}\text{N}(001)/\text{MgO}(001)$ with $x = 0-1$. Figure 1(α) and 1(β) show generic RHEED patterns for an MgO(001) substrate. As can be seen from Fig. 1, RHEED shows that the $\text{Sc}_x\text{Ga}_{1-x}\text{N}(001)$ growth is epitaxial for all values of x . The ScGaN film has a clearly crystalline structure at each value of x , and there is a cube-on-cube epitaxial relationship with the substrate, as $[110]_{\text{ScGaN}} \parallel [110]_{\text{MgO}}$ and $[100]_{\text{ScGaN}} \parallel [100]_{\text{MgO}}$. Despite the fact that GaN is zinc-blende and ScN is rock-salt, both have fcc crystal structure. This can be considered the reason why the RHEED patterns at all values of x along a given azimuth (α or β) display the same reciprocal space symmetry. From the RHEED patterns of Fig. 1, one feature stands out clearly as a function of x . Namely, as x increases, the RHEED pattern becomes noticeably brighter at around $x = 0.5$. This may be interpreted as an effect of the surface structure and surface stoichiometry. Whereas GaN(001) growth proceeds well under Ga-rich conditions with excess Ga adatoms, leading to a partly diffusive RHEED pattern, ScN(001) grows smoothly under either Sc-rich or N-rich conditions without accumulating more than 1 monolayer of Sc adatoms, thus leading to a more distinctive RHEED pattern [2, 5, 6]. These growth modes are closely tied to the underlying crystal structure of the surface, zinc-blende vs. rock-salt. It is therefore clear that as x increases, the growth transitions from zinc-blende structure at small x to rock-salt structure at large x . The transition point appears to be in the vicinity of $x = 0.5$, at which point the RHEED pattern becomes noticeably brighter compared to at $x = 0.25$.

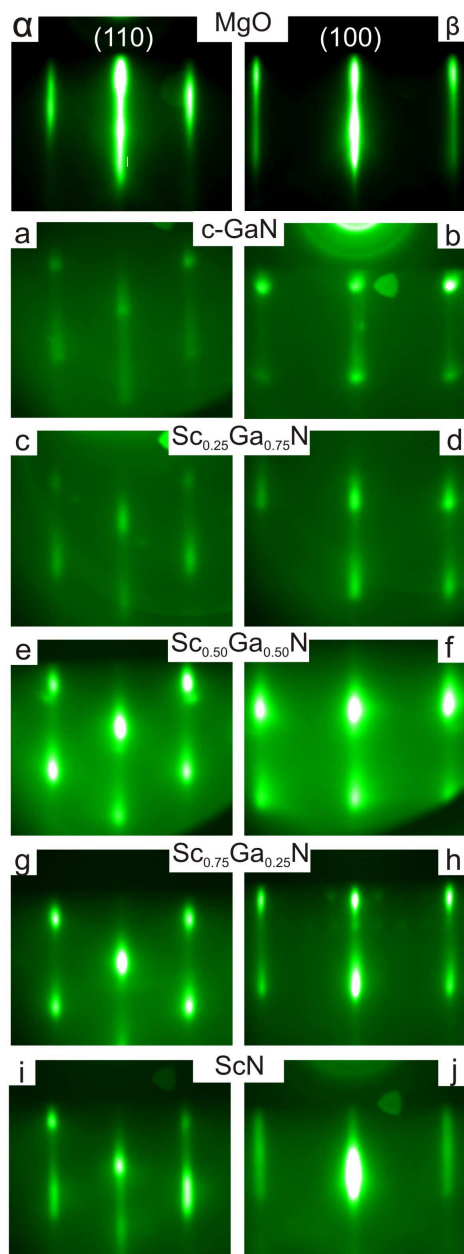


Figure 1 (α) RHEED pattern of MgO(001) substrate along [110]; (β) RHEED pattern of MgO(001) substrate along [100]; (a) – (j) RHEED patterns for $\text{Sc}_x\text{Ga}_{1-x}\text{N}(001)/\text{MgO}(001)$ with $x = 0 - 1$; images (a), (c), (e), (g), and (i) are taken along same azimuth as (α); images (b), (d), (f), (h), and (j) are taken along same azimuth as (β).

Shown in Fig. 2 are RHEED patterns of ScGaN growth on sapphire(0001) [10]. For these values of $x = 0.54$ and 0.78 , the RHEED pattern is similar to that of ScN(111) along [1-10] but with also the development of a ring-like structure, indicating polycrystalline ScGaN (111)-oriented grains. Comparing this to the growth at $x = 0.5$ and 0.75 on MgO(001) [see Fig. 1(e) and 1(g)], we see that the growth on MgO with (001) orientation is of significantly better quality in that it does not develop such polycrystallinity. This is clearly an advantage of the (001)-oriented growth.

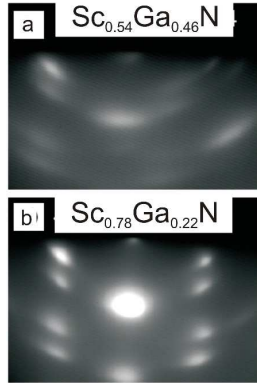


Figure 2 (a) and (b) RHEED patterns of Sc_xGa_{1-x}N/sapphire(0001) with $x = 0.54$, and 0.78 , respectively (image reproduced from Ref. 10).

In Fig. 3 we present a portion of the XRD data ($39^\circ - 41^\circ$) for c-GaN, Sc_{0.25}Ga_{0.75}N, Sc_{0.50}Ga_{0.50}N, Sc_{0.75}Ga_{0.25}N, and ScN films. The XRD data presented in Fig. 3 was calibrated using the MgO 002 peak of the substrate (not shown here) with $2\theta = 42.94^\circ$ which gives a lattice constant of $a_{\text{MgO}} = 0.4213$ nm. In Fig. 3, one can observe that there are peak shifts. For example, the 002 peak shifts to the right by $\sim 0.07^\circ$ from $2\theta = 39.81(6)^\circ$ (c-GaN) to $2\theta = 39.88(6)^\circ$ (Sc_{0.25}Ga_{0.75}N). As the Sc concentration is increased to 50% the peak shifts to $2\theta = 39.96(6)^\circ$ (Sc_{0.50}Ga_{0.50}N peak). At 75%, the 002 peak is at $2\theta = 39.95(2)^\circ$ (Sc_{0.75}Ga_{0.25}N peak). Finally, the ScN peak is found at $2\theta = 39.96(3)^\circ$. It is worth noting that the peak for Sc_{0.75}Ga_{0.25}N film is very close to the ScN peak ($\sim 0.01^\circ$ difference). This small difference between Sc_{0.75}Ga_{0.25}N and ScN clearly indicates that the crystal structure preferred by Sc_{0.75}Ga_{0.25}N is rock-salt – the same as ScN.

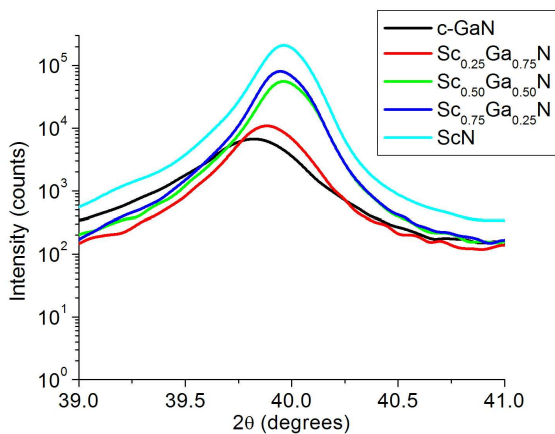


Figure 3 XRD data plots of c-GaN, Sc_{0.25}Ga_{0.75}N, Sc_{0.50}Ga_{0.50}N, Sc_{0.75}Ga_{0.25}N, and ScN on MgO(001) in the range $2\theta = 39 - 41^\circ$. The peaks shown are the 002 peaks.

We calculated the out-of-plane (a_\perp) lattice constant using Bragg's law. The XRD data was first calibrated to the MgO peak as mentioned above. We used a value of $\lambda = 0.1542$ nm for the average wavelength of our Cu $K_{\alpha 1}$ and $K_{\alpha 2}$ x-rays. The a_\perp and layer thickness values are presented in Table I.

Table I Layer thickness (t_{ScGaN}), and out-of-plane (a_{\perp}) lattice constant values for $\text{Sc}_x\text{Ga}_{1-x}\text{N}$ at various x compositions ($0 \leq x \leq 1$).

Composition x	t_{ScGaN} (nm)	a_{OUT} (nm)
0	187	0.4529
0.25	80	0.4521
0.50	280	0.4512
0.75	430	0.4514
1	495	0.4513

The evolution of the a_{\perp} lattice constants as a function of Sc concentration x can be observed in Fig. 4. Our measured a_{\perp} lattice constants for c-GaN (0.4529 nm), and ScN (0.4513 nm) are in very good agreement with previously reported value of 0.4530 nm [2], and 0.4501 nm [6], respectively. It is interesting to note that the a_{\perp} lattice constant values for c-GaN, $\text{Sc}_{0.25}\text{Ga}_{0.75}\text{N}$, and $\text{Sc}_{0.50}\text{Ga}_{0.50}\text{N}$ decrease linearly with x (from 0.4529 to 0.4512 nm). This linear behavior clearly suggests that $\text{Sc}_{0.25}\text{Ga}_{0.75}\text{N}$ has the same zinc blende crystal structure as c-GaN. The $\text{Sc}_{0.50}\text{Ga}_{0.50}\text{N}$ film seems to be close to a transition point, as also observed in Fig. 1. As the scandium concentration is increased from 50% to 75% and then to 100%, a_{\perp} is fairly constant with x , which suggests rocksalt structure over most of this range. So far, our preliminary results agree reasonably well with recent theoretical calculations of Zerroug *et al.* [11] who predicted that for Sc concentrations of 0%, 25%, and 50%, the zinc blende structure is more favorable than the rocksalt structure, whereas for Sc concentrations of 75% and 100%, the rocksalt structure is the most stable configuration with respect to zinc blende structure. Our measured lattice constants of zinc-blende GaN (0.4529 nm), and rock-salt ScN (0.4513 nm), do not agree very well with the corresponding 0.455 nm and 0.454 nm lattice constants obtained by Zerroug *et al.* Furthermore, the point at $x = 0.5$ cannot be concluded from our experiment to correspond to zinc-blende structure, as the RHEED data suggests the possibility of rock-salt.

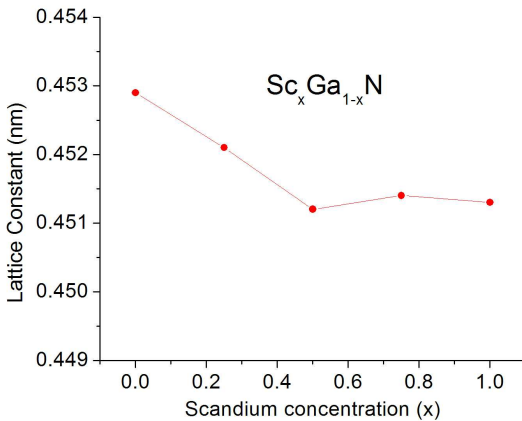


Figure 4 Out-of-plane (a_{\perp}) lattice constants as a function of Sc concentration x .

CONCLUSIONS

ScGaN has been grown with a range of stoichiometry from $x = 0$ (ZB-GaN) to $x = 1$ (RS-ScN). The results indicate that the range of x up to ~ 0.5 has ZB structure, whereas the range beyond 0.5 has RS structure. The exact location of the transition point seems to be near $x = 0.5$. Further studies are in progress to explore the in-plane lattice parameter variations as a function of x and to correlate this with the out-of-plane variations described here.

ACKNOWLEDGMENTS

Funding for this study was provided by the Department of Energy, Office of Basic Energy Sciences (Grant No. DE-FG02-06ER46317) and by the National Science Foundation (Grant No. 0730257).

REFERENCES

- [1] M. B. Haider, R. Yang, C. Constantin, E. Lu, A. R. Smith, and H. A. H. Al-Britthen, *J. Appl. Phys.* **100**(08), 083516 (2006).
- [2] H. A. AL-Britthen, R. Yang, M. B. Haider, C. Constantin, E. Lu, A. R. Smith, N. Sandler, P. Ordejón, *Phys. Rev. Letters* **95**, 146102 (2005).
- [3] W. R. Lambrecht1, *Phys. Rev. B* **62**, 13538 (2000).
- [4] C. Stampfl, W. Mannstadt, R. Asahi, and A. J. Freeman, *Phys. Rev. B* **63**, 155106 (2001).
- [5] H. A. Al-Britthen, E. M. Trifan, D. C. Ingram, A. R. Smith, and D. Gall, *J. Cryst. Growth* **242**, 345 (2002).
- [6] A. R. Smith, H. A. H. Al-Britthen, D. C. Ingram, and D. Gall, *J. Appl. Phys.* **90**, 1809 (2001).
- [7] D. Gall, I. Petrov, L. D. Madsen, J. E. Sundgren, and J. E. Greene, *Vac. Sci. Technol. A* **16**, 2411 (1998).
- [8] C. Constantin, M. B. Haider, D. Ingram, A. R. Smith, N. Sandler, K. Sun, and P. Ordejón, *J. Appl. Phys.* **98**(12), 123501 (2005).
- [9] C. Constantin, M. B. Haider, D. Ingram, and A. R. Smith, *Appl. Phys. Lett.* **85**(26), 6371 (2004).
- [10] C. Constantin, H. Al-Britthen, M. B. Haider, D. Ingram, and A. R. Smith, *Phys. Rev. B* **70**, 193309 (2004).
- [11] S. Zerroug, F. Ali Sahraoui, and N. Bouarissa, *J. of Appl. Phys.* **103**, 063510 (2008).